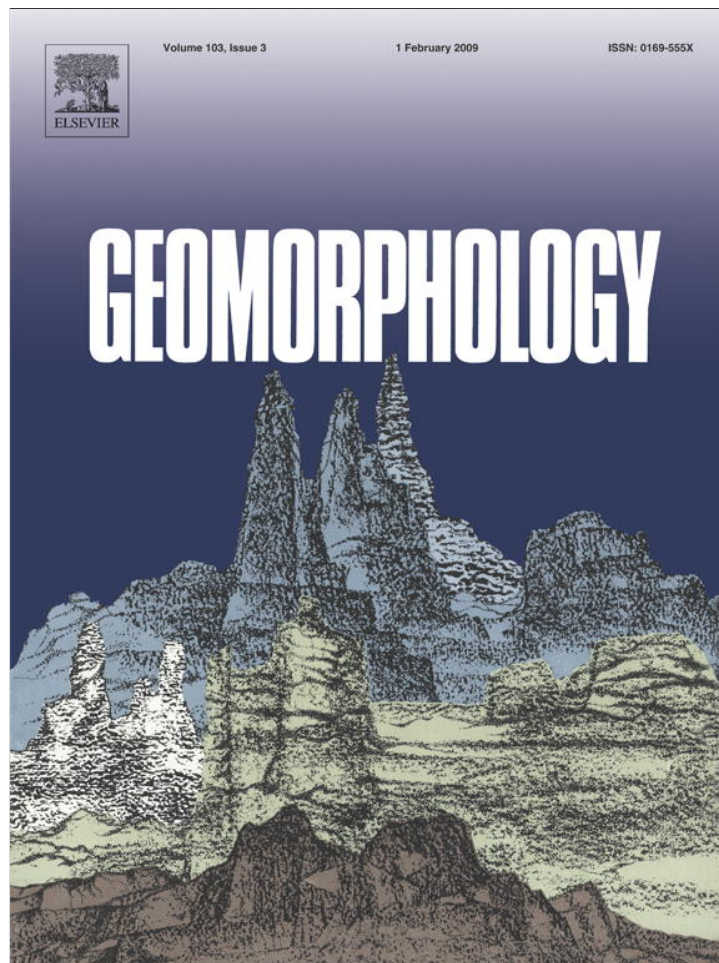


Provided for non-commercial research and education use.
Not for reproduction, distribution or commercial use.



This article appeared in a journal published by Elsevier. The attached copy is furnished to the author for internal non-commercial research and education use, including for instruction at the authors institution and sharing with colleagues.

Other uses, including reproduction and distribution, or selling or licensing copies, or posting to personal, institutional or third party websites are prohibited.

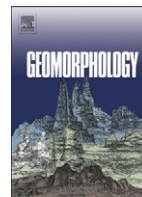
In most cases authors are permitted to post their version of the article (e.g. in Word or Tex form) to their personal website or institutional repository. Authors requiring further information regarding Elsevier's archiving and manuscript policies are encouraged to visit:

<http://www.elsevier.com/copyright>



Contents lists available at ScienceDirect

Geomorphology

journal homepage: www.elsevier.com/locate/geomorph

Destabilization of streambanks by removal of invasive species in Canyon de Chelly National Monument, Arizona

Natasha Pollen-Bankhead^{a,*}, Andrew Simon^a, Kristin Jaeger^b, Ellen Wohl^b

^a USDA-ARS National Sedimentation Laboratory, P.O. Box 1157, Oxford, MS 38655, USA

^b Department of Geosciences, Colorado State University, Ft. Collins, CO 80523, USA

ARTICLE INFO

Article history:

Received 21 March 2008

Received in revised form 7 July 2008

Accepted 8 July 2008

Available online 16 July 2008

Keywords:

Streambank stability

Riparian vegetation

Invasive species

Tamarisk

American Southwest

ABSTRACT

As part of a study to investigate the causes of channel narrowing and incision in Canyon de Chelly National Monument, the effects of Tamarisk and Russian-olive on streambank stability were investigated. In this study, root tensile strengths and distributions in streambanks were measured and used in combination with a root-reinforcement model, RipRoot, to estimate the additional cohesion provided to layers of each streambank. The additional cohesion provided by the roots in each 0.1-m layer ranged from 0 to 6.9 kPa for Tamarisk and from 0 to 14.2 kPa for Russian-olive. Average root-reinforcement values over the entire bank profile were 2.5 and 3.2 kPa for Tamarisk and Russian-olive, respectively.

The implications of vegetation removal on bank stability and failure frequency were evaluated in two incised reaches by modeling bank-toe erosion and bank stability with and without vegetation. The effects of a series of 1.0- and 1.5-m-deep flows on bank-toe erosion, pore-pressure distributions, and bank stability were evaluated first. In addition, bank stability model runs were conducted using iterative modeling of toe erosion and bank stability using a discretized flow and groundwater record for one year. Results showed that the effects of root-reinforcement provided by Tamarisk and Russian-olive have a significant impact on bank-stability and bank-failure frequency. Because the bank materials are dominated by sands, cohesion provided by roots is significant to bank stability, providing an average 2.8 kPa of cohesion to otherwise cohesionless bank materials. Bank retreat rates at one site following vegetation removal have approximately doubled when compared to the control reach (from an approximate rate of 0.7–0.8 m/y between 2003 and 2006 to 1.85 m/y during the year modeled). Vegetation removal along the entire riparian corridor in Canyon de Chelly may lead to the introduction of significantly more sediment to the system through bank widening processes, although it is not known whether this change alone would be sufficient to cause a shift in channel morphology to the wide-braided channels that were once characteristic of this canyon.

Published by Elsevier B.V.

1. Introduction

The natural disturbance regime of arid and semiarid sand-bedded stream channels is characterized by cycles of large floods causing substantial channel widening followed by channel narrowing during floods of smaller magnitude (Schumm and Lichty, 1963; Osterkamp and Costa, 1987). In these cycles, large floods with recurrence intervals of between 20 and 300 years, reset narrow, meandering channels to a wide, shallow, and often braided morphology (Schumm and Lichty, 1963; Osterkamp and Costa, 1987). Following such large floods, channel narrowing takes place over several decades, as a result of low flows with insufficient stream power to rework the entire channel. As the active channel narrows, the bed incises and channel morphology

remains narrow until the occurrence of another large flood returns the channel to a wide and braided morphology.

One aspect of this channel narrowing is the ability of riparian vegetation to establish within and adjacent to the channel, which helps to stabilize portions of the once-active channel. The presence of vegetation increases hydraulic roughness, facilitates sediment deposition (Hupp and Osterkamp, 1996; Tooth and Nanson, 1999, 2000) and strengthens the bank through root-reinforcement (Abernethy and Rutherford, 2001; Pollen and Simon, 2005; Pollen, 2007) thereby creating a positive feedback. In the American Southwest, floodplain vegetation was historically dominated by Fremont cottonwood (*Populus fremontii*), Goodding willow (*Salix gooddingii*), and sandbar willow (*Salix exigua*) (Birken and Cooper, 2006). During the twentieth century, however, invasive exotic species such as Tamarisk (*Tamarix ramosissima*) and Russian-olive (*Elaeagnus angustifolia*) began to proliferate and now dominate many riparian zones in the southwest USA (Friedman et al., 2005). Replacement of native vegetation by Tamarisk and Russian-olive along channel banks may inhibit the channel's ability to shift morphology from single-thread meandering to braided. Tamarisk has been found to be

* Corresponding author. Tel.: +1 662 232 2918; fax: +1 662 281 5706.

E-mail addresses: natasha.bankhead@ars.usda.gov (N. Pollen-Bankhead), andrew.simon@ars.usda.gov (A. Simon), kljaeger@warnerncr.colostate.edu (K. Jaeger), ellenw@warnerncr.colostate.edu (E. Wohl).

more drought tolerant compared to native cottonwood and therefore has a competitive advantage (Busch and Smith, 1995). In addition, Tamarisk stands have a higher stem density than cottonwood and therefore have greater hydraulic roughness, which decreases local flow velocities and allows it to be more resistant to removal by large floods. Because channel banks supporting Tamarisk are more resistant to erosion, occurrence of overbank flooding is increased during moderate flows (Graf, 1978). Overbank flooding combined with increased hydraulic roughness caused by vegetation facilitates increased vertical sediment deposition along banks and serves as a feedback to further narrowing of the channel (Schumm and Lichty, 1963; Friedman et al., 2005).

In Canyon de Chelly National Monument in northeastern Arizona, increased channel narrowing and incision have been occurring during the past century, similar to other drainages within the southern Colorado Plateau. These channel changes have been attributed to a number of factors, including climatic and anthropogenic changes in the flow regime and the coincidental timing of the invasion of the exotic riparian species (Everitt, 1980; Cadol, 2007). The study area has been subject to overgrazing since the 1700s, with peak intensity in livestock numbers occurring in the 1800s. It is estimated that 80 to 90% of Arizona range land remains in a degraded state today, despite the fact that livestock numbers had fallen by the 1940s (McPherson, 1998; Weisiger, 2000; Travis, 2007). Degradation of the range land includes trampled surfaces, destroyed cryptobiotic crusts, and the prevalence of exotic trees, grasses and shrubs.

The National Park Service (NPS) is currently engaged in an experimental program to remove the invasive species Tamarisk and Russian-olive from the margins of Canyon de Chelly, Arizona. The objective of this program is to return the channels to the wide and shallow geometry characteristic of the region a century ago by making banks more susceptible to erosion. More frequent bank-toe erosion and failures would then result in channel widening with the failed sediment serving to aggrade the channel bed.

The NPS invasive removal program includes a total of six 1.1-km-long plots located throughout the national monument. Four plots are located in Canyon de Chelly and two in Canyon del Muerto. Each plot consists of a 300-m-long control reach located at the upstream end, followed by a 300-m reach with aboveground plant removal treatment (using herbicide), and a further 300-m reach with above- and belowground plant removal treatment (trees were cut with a chainsaw, the slash burned, and the roots removed using a backhoe). Approximately 200 m of channel separates the two plant removal treatments in each reach.

2. Purpose and scope

The purposes of this study were to quantify the additional strength provided to streambanks by root-reinforcement from Tamarisk and Russian-olive, and to determine how the loss of this strength impacts the frequency of bank failures. Work was concentrated in two incised reaches of Canyon de Chelly known as Upper White House (UWH) and Sliding Rock (SLR) (Fig. 1). Of the six 1.1-km reaches, the Upper White House site was the first to undergo vegetation removal treatments (one 300-m reach of aboveground plant removal by herbicide and one 300-m reach with above and belowground plant removal), in spring and summer of 2006. At the time of field data collection for this study, vegetation removal had not yet begun at Sliding Rock, and thus rates of widening over the period of investigation could be compared for one site that had been modified (UWH) and one that had been left untreated (SLR).

3. Methods

3.1. Root-reinforcement

Root tensile strengths for Tamarisk and Russian-olive were measured using a device called the Root-Puller, based on a design by Abernethy and Rutherford (2001). This is comprised of a metal frame with a winch

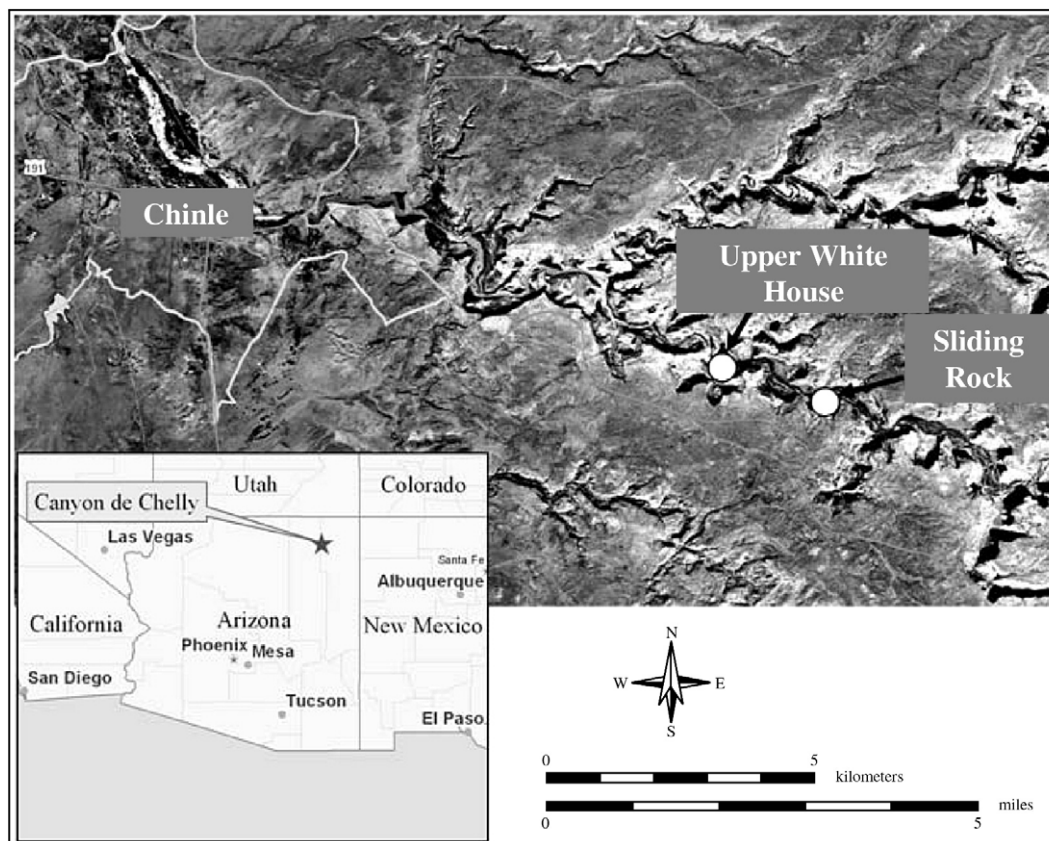


Fig. 1. Location map of Canyon de Chelly National Monument, Arizona, and the two study reaches.

attached to a load cell and displacement transducer and both connected to a Campbell CR510 data logger. The Root-Puller is attached to the bank face and different-sized roots. Cranking the winch applies a tensile stress to the root (measured as a load, in Newtons) that increases until tensile failure of the root occurs. The diameter of each root is recorded along with the logged history of tensile stress and shear displacement. The maximum load applied to each root before breaking and root diameter were used to calculate the tensile strength of each root. Root diameter–tensile strength relations were established for the two species to use as input to the fiber–bundle root–reinforcement model, RipRoot (Pollen and Simon, 2005; Pollen, 2007). Root systems of the two species were also examined and recorded using the wall-profile method (Bohm, 1979).

Root diameters were measured and recorded according to depth in the bank profile. Estimates of the increase in strength (ΔS) provided by the roots of each species at varying depths were calculated using the root-architecture and tensile-strength data that were collected and input into the RipRoot model, which accounts for the progressive breaking of roots and corrects for the overestimation of ΔS typical of earlier models (i.e., Wu et al., 1979).

Geotechnical properties of the banks were measured *in situ* with an Iowa Borehole Shear Tester. Samples of bank materials were taken for each stratigraphic layer at each site, and sieved to half-Phi intervals in the laboratory to obtain particle size distributions for bank stability and toe erosion algorithms. In addition, cross-sectional surveys were carried out at the sites at the beginning and end of the modeled period to provide bank geometry information to input in the streambank stability model (BSTEM 4.1; Simon et al., 2000) and to validate the modeling results.

3.2. Bank stability and failure frequency

To investigate the relative stability of the streambanks with and without vegetation, Version 4.1 of the bank-stability and toe-erosion model originally developed by Simon et al. (2000) was used. The model is a Limit Equilibrium analysis in which the Mohr–Coulomb failure criterion is used for the saturated part of the wedge, and the Fredlund et al. (1978) criterion is used for the unsaturated part. These criteria indicate that apparent cohesion changes with matric suction, whereas effective cohesion remains constant. In addition to accounting for positive and negative pore-water pressures, the model incorporates complex geometries, layered soils, changes in soil unit weight based on moisture content, and external confining pressure from streamflow. The model divides the bank profile into five user-definable layers with unique geotechnical properties. The Factor of Safety (F_s) is given by

$$F_s = \frac{\sum_{i=1}^I (c'_i L_i + S_i \tan \phi_i^b + [W_i \cos \beta - U_i + P_i \cos(\alpha - \beta)] \tan \phi_i^c)}{\sum_{i=1}^I (W_i \sin \beta - P_i \sin[\alpha - \beta])} \quad (1)$$

where c'_i =effective cohesion of the i th layer (kPa), L_i =length of the failure plane incorporated within the i th layer (m), S_i =force produced by matric suction on the unsaturated part of the failure surface (kN/m), W_i =weight of the i th layer (kN), U_i =the hydrostatic-uplift force on the saturated portion of the failure surface (kN/m), P_i =the hydrostatic-confining force from external water level (kN/m), β =failure-plane angle (degrees from horizontal), α =bank angle (degrees from horizontal), and I =the number of layers. The angle ϕ^b describes the rate of increase in shear strength with increasing matric suction.

Failure plane length is determined using the failure plane angle and the point of emergence of the failure surface on the bank face or bank toe. Past iterative runs using BSTEM have indicated that for planar failures with a straight bank face, the most critical failure planes emerge at the top of the bank toe. For cantilever failures involving undercut banks, the most critical failure planes tend to occur through the point of greatest undercutting. Failure surface angles can

be approximated from past failures at the field site of interest, or by using the average of the soil friction angle and average bank angle. For more complex bank geometries, failure surface angles and block geometries can, however, vary from these general cases. As such, the observations noted above were used as a starting point for finding critical failure surfaces in the banks modeled in this study, but different failure angles and emergence points were checked for lower, more critical factor of safety values.

An excess shear-stress approach and a simplified, rectangular-shaped hydrograph is used to simulate bank-toe erosion. The mean boundary shear stress (τ_o) operating on the bank material is represented by

$$\tau_o = \gamma R S \quad (2)$$

where τ_o is the applied shear stress (Pa), γ is unit weight of water (N/m³), R is local hydraulic radius (m), and S is channel slope (m/m).

The average boundary shear stress exerted by the flow on each node is determined by dividing the flow area at a cross-section into segments that are affected only by the roughness of the bank or bed and then further subdividing to determine the flow area affected by the roughness of each node. The line dividing the bed- and bank-affected segments is assumed to bisect the average bank angle and the average bank toe angle. The hydraulic radius of the flow on each segment is the area of the segment divided by the wetted perimeter of the segment.

It is assumed that flow is uniform and that no plant stems are present to create drag forces. In this case, the two sites studied are situated at the downstream exit of two separate meander bends, on the outer banks. As such, the assumption of uniform flow may slightly underestimate the mean boundary shear stresses used in the toe erosion algorithm. Sinuosity of the channel is however, low, so although this potential underestimation is recognized, it is not perceived to be a major limitation in this study.

It should be made clear that the BSTEM model is not a channel evolution model, and does not route flow and sediment. The bed is also assumed to be fixed. As such, incision cannot be predicted using the model, only bank retreat. In addition, the influence of sediment load coming from upstream on the erosion rate is not considered; once mass failure of a bank has occurred, the failed material is assumed to be automatically entrained by the flow in the channel. The line dividing the bed- and bank-affected segments is assumed to bisect the average bank angle and the average bank-toe angle. The hydraulic radius of the flow on this segment is the area of the segment (A) divided by the wetted perimeter of the segment (P_n), and S is the channel slope. An average erosion distance is computed by assuming that the rate of erosion ε (in m/s) is proportional to the shear stress in excess of the critical shear stress (Partheniades, 1965; Simon and Thomas, 2002):

$$\begin{aligned} \varepsilon &= k(\tau_o - \tau_c)^a && \text{(for } \tau_o > \tau_c) \\ \varepsilon &= 0 && \text{(for } \tau_o \leq \tau_c) \end{aligned} \quad (3)$$

where ε =erosion flux (m s⁻¹); k =erodibility coefficient (cm³ N⁻¹ s⁻¹); $(\tau_o - \tau_c)$ =excess shear stress (Pa); τ_o =toe material shear stress (Pa); τ_c =critical shear stress (Pa); and a =an exponent (often assumed=1.0).

Erosion is then calculated as a function of the amount of time that the bank-toe materials are experiencing shear stresses in excess of the critical values of the material. Jet test results have previously been used to develop a relation between critical shear stress (τ_c) and the erodibility coefficient (k) (Hanson and Simon, 2001). Hanson and Simon (2001) found an inverse relationship between τ_c and k , where soils exhibiting a low τ_c have a high k , and soils having a high τ_c tend to have a low k . Based on their observations, k can be estimated as a function of τ_c ($R^2=0.60$):

$$k \approx 0.1 \tau_c^{-0.5} \quad (4)$$

Two methods were employed to model the effects of vegetation removal on bank stability and erosion rates in Canyon de Chelly. First,

the annual hydrograph was analyzed to determine the typical occurrence of 1.0- and 1.5-m flows, which both occurred several times during the period of time to be modeled (July 2006 to July 2007). The effects of a series of 1.0- and 1.5-m flows on bank-toe erosion, pore-pressure distributions, and bank stability were then evaluated using BSTEM 4.1 (Simon et al., 2007). Stability analyses were conducted with and without vegetation for the failure conditions at peak flow (equal flow and groundwater elevations) and for the drawdown condition following recession of stage where the heightened groundwater levels were maintained. Two sites (UWH and SLR) were modeled using surveys from summer 2006 to determine bank profiles before vegetation was removed.

Second, an annual flow hydrograph from a stage gage set up 1 km downstream of the UWH site was discretized into individual storm events, with each event split into three sections to determine flow depth during rising, peak and recession elements of each storm hydrograph and their duration. Groundwater measurements from wells installed at each site were paired with each of the discretized flow depths and run in BSTEM 4.1 to simulate bank-toe erosion, pore-pressure distributions, and bank stability as in the first set of runs. As before, simulations were carried out with and without vegetation. The UWH and SLR sites were modeled using surveys from summer 2006,

before vegetation removal and bank grading occurred at the UWH site. In addition, the regraded bank profile at UWH was modeled. For this second set of model runs, the predicted erosion over the modeling period was compared with actual erosion calculated between summer 2006 and summer 2007 surveys. The BSTEM model was run in a series of iterative steps until all of the flow events were simulated using the following set of steps:

- i. The effects of the first flow event was simulated using the toe-erosion submodel to determine the amount (if any) of hydraulic erosion and the change in geometry in the bank-toe region.
- ii. The new geometry was exported into the bank-stability submodel to test for the relative stability of the bank.
 - a. If the factor of safety (F_s) was >1.0 , geometry was not updated and the next flow event was simulated.
 - b. If F_s was <1.0 , failure was simulated and the resulting failure plane became the geometry of the bank for simulation of toe erosion for the next flow event in the series.
 - c. If the next flow event had an elevation lower than the previous one, the bank-stability submodel was run again using the new flow elevation to test for stability under drawdown conditions (Fig. 8). If F_s was <1.0 , failure was

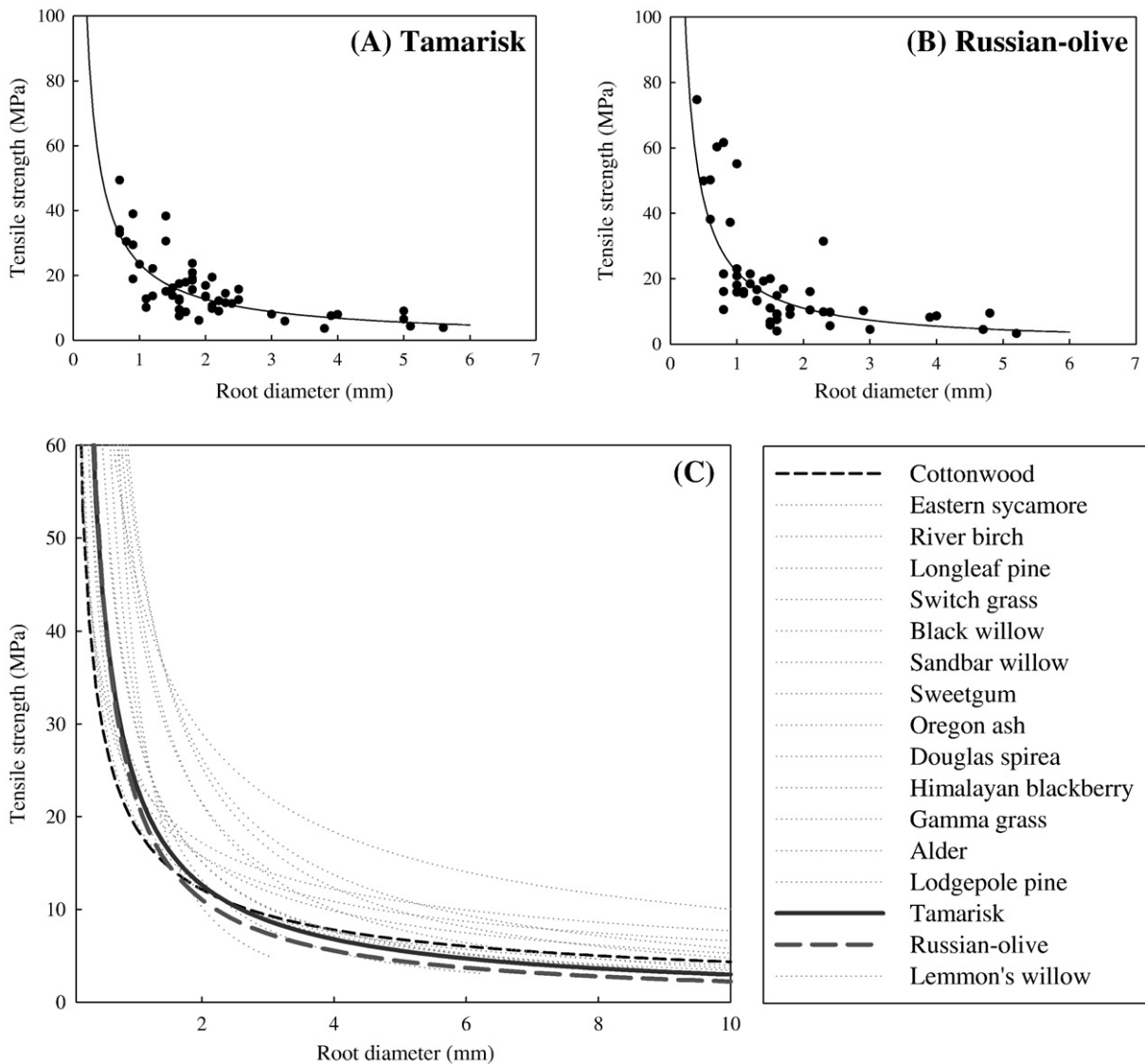


Fig. 2. Root tensile-strength measurements for Tamarisk (A) and Russian-olive (B) and relations for these species compared to other riparian species tested by the authors (C). To distinguish the specific curves of other species see Simon and Collison (2002), Pollen and Simon (2005), Simon et al. (2006).

simulated and the new bank geometry was exported into the toe-erosion submodel for the next flow event.

iii. The next flow event in the series was simulated.

Volumes of sediment erosion by hydraulic and geotechnical processes and the number of mass failures were noted for each flow event and bank-stability simulation. As the bank-stability submodel provides calculations of the amount of failed material in two dimensions (m²), a reach length of 100 m was assumed for all simulations to provide eroded volumes in m³. Values were summed for all events to obtain the amount of erosion under the prevailing conditions.

4. Results and discussion

4.1. Root-reinforcement

Relations between tensile strength and diameter for Tamarisk and Russian-olive (Fig. 2A and B) were developed from field testing and were similar to other woody, riparian species (Simon and Collison, 2002; Pollen and Simon, 2005; Simon et al., 2006) (Fig. 2C):

$$\text{Tamarisk : } T = 23.6 d^{-0.9} \quad (5)$$

$$\text{Russian-olive : } T = 22.1 d^{-1.0} \quad (6)$$

where T =tensile strength (megapascals; MPa) and d =root diameter (mm). The lines of best fit for the two species indicate that the tensile strength of roots in the 0.1- to 2.0-mm-diameter range tends to fall in the middle of the values found to be typical for riparian species tested all over the USA, but roots of larger diameter tended to be at the lower end of the strength range measured for other riparian species (Fig. 2C). Where the roots of other riparian species tend to be concentrated in the top 1 m of the soil profile, roots of Tamarisk and Russian-olive in this semiarid environment extend throughout the bank profile to obtain water from greater depths (up to 4.3 m in these investigations). The additional cohesion provided by the roots in each 0.1-m layer ranged from 0 to 6.9 kPa for Tamarisk and from 0 to 14.2 kPa for Russian-olive.

Average root-reinforcement values over the entire bank profile were 2.5 and 3.2 kPa for Tamarisk and Russian-olive, respectively.

The bank stability algorithms in BSTEM are most sensitive to changes in soil cohesion and pore-water pressure (Langendoen and Simon, 2008), and as such, changes in cohesion due to different soil types and/or roots are particularly important. Because in this case the bank materials are dominated by sands, cohesion provided by roots is particularly significant to bank stability, providing an average 2.8 kPa of cohesion to otherwise cohesionless bank materials (Fig. 3). Cohesion values for bank materials range from 0 kPa for sands and gravels to approximately 15 kPa for stiff clays (Selby, 1982). Cohesion provided by roots, therefore, have a greater relative effect on sands and silts than stiff clays.

Root distributions appeared to be largely affected by the layering within the bank profiles. Noticeably higher root-area-ratio (RAR) values were concentrated at depths within the bank corresponding to changes in stratigraphy and bank material type. This may be because water often accumulates at stratigraphic contacts. In addition, Russian-olive and Tamarisk trees studied in Canyon de Chelly show periods of time during which burial occurred and resulting bank stratigraphy and concentrations of roots may be a feature of progressive periods of burial by sediment.

4.2. Bank stability and predicted failure frequency

Analysis of changes in bank stability for the UWH and SLR reaches was conducted using the Bank Stability and Toe Erosion Model (Simon et al., 2000) populated with geotechnical properties of the banks with and without vegetation (Table 1; Fig. 4). Banks in the UWH and SLR sections are 4.3 and 3.9 m high, respectively, and are dominated by sand except near the toe where fine-grained deposits provide between 2.2 and 4.0 kPa of cohesion. Initial model setup conditions (with vegetation) showing bank layering, the potential failure plane, and stable F_s (>1.0) are shown with the associated channel geometry for both reaches (Fig. 4).

First the effects of a series of 1.0- and 1.5-m-deep flows were simulated. These flow depths were selected as they occur on a reasonably frequent basis in Canyon de Chelly (Fig. 5); during the time period modeled (July 2006–May 2007), flows of between 1.0 and 1.5 m occurred three times and flows > 1.5 m occurred twice (Fig. 5). Analysis of the precipitation record in

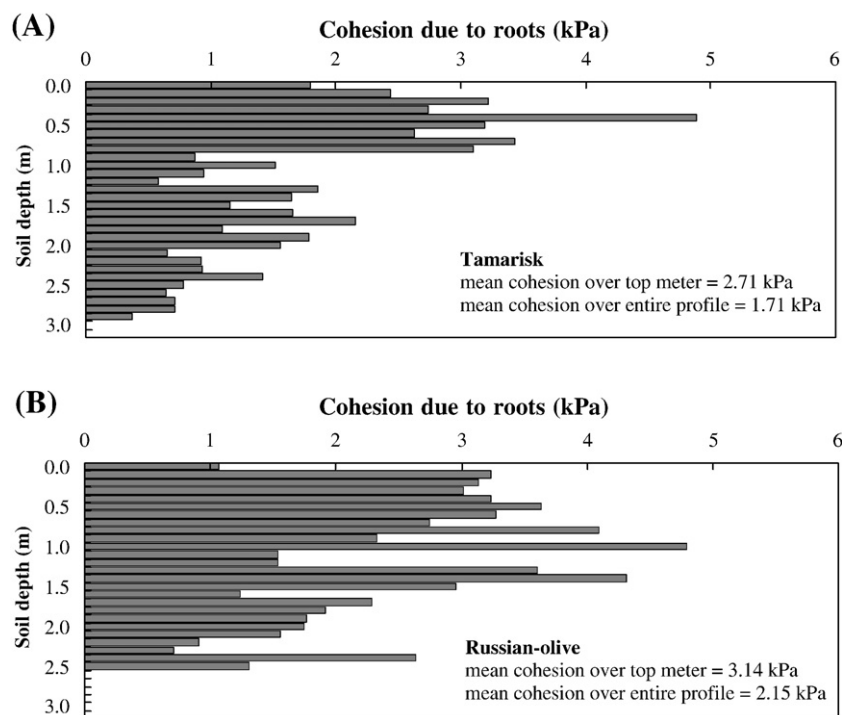


Fig. 3. Average values for cohesion from roots in each 0.1-m soil layer for Tamarisk (A) and Russian-olive (B).

Table 1

Geotechnical properties assigned to each bank layer based on borehole shear tests of bank materials and cohesion from root-reinforcement of Russian-olive and Tamarisk for the two study reaches

Reach	Condition	Bank layer									
		1		2		3		4		5	
		c'	ϕ'	c'	ϕ'	c'	ϕ'	c'	ϕ'	c'	ϕ'
Upper White House	No vegetation	0.0	34.5	0.0	38.6	3.0	20.9	0.0	35.5	2.2	20.9
	With vegetation	2.5	34.5	1.9	38.6	5.1	20.9	3.1	35.5	5.3	20.9
Sliding Rock	No vegetation	0.0	34.5	0.0	38.6	2.4	28.4	0.0	28.4	4.0	28.4
	With vegetation	2.2	34.5	2.4	38.6	6.0	28.4	3.0	28.4	7.0	28.4

Note: cohesion, c' in kPa, friction angle, ϕ' in degrees.

Canyon de Chelly indicated that the total annual precipitation for 2006 represented the 40th percentile for annual precipitation over the 88-year record. This is therefore close to the average for the period of precipitation measurement in Canyon de Chelly (Fig. 6).

Toe erosion was simulated for a specified flow with the eroded geometry exported into the bank-stability part of the model where F_s was calculated for peak-flow and drawdown conditions. Direct measurements of τ_c and k were not possible at the field sites in Canyon de Chelly using a jet-test device (Hanson, 1990), because of difficulties with site accessibility and water supply. Critical shear stress (τ_c) of the cohesive materials was, therefore, set between 1.5 and 3 Pa with associated erodibility coefficients (k) of 0.082 and 0.058 $\text{cm}^3/\text{N}\cdot\text{s}$ (Hanson and Simon, 2001), based on percent sand, silt, and clay of samples taken at each site. For sands, τ_c was set at 0.5 Pa and k at 0.141 $\text{cm}^3/\text{N}\cdot\text{s}$ (Hanson and Simon, 2001). Several studies of soil erodibility and measurement of τ_c and k have, however, shown that values can vary up to several orders of magnitude even at the same site (Wynn and Mostaghimi, 2006; Gordon et al., 2007; Knapen et al., 2007). Indeed, the relation from Hanson and Simon (2001) given in Eq. (4) has an r^2 of 0.6, indicating a considerable amount of scatter about the regression line. Using the regression in Eq. (4) to obtain values for τ_c and k in the absence of field data may therefore lead to a degree of error in these variables, which should be taken into account when analyzing the results.

With the added cohesion provided by the vegetation, these banks remained stable until the seventh 1.0-m flow or the second 1.5-m flow (Table 2). Without vegetation to reinforce the banks, failure was simulated to occur during recession of the fourth 1.0-m flow or at the peak of the first 1.5-m flow. Given a consistent flow-frequency regime, these results indicate that bank failures at the UWH site will occur at more than twice the frequency as they occur today with the vegetation in place. Results were more dramatic for the SLR site where for 1.0-m flows failure was simulated on recession for the vegetated case during the fifth event compared to the recession of the first event for the unvegetated case.

In the second set of model runs, the discretized flow record was used (Fig. 5). In terms of rainfall, the monsoon season of 2006 (July and August) was wetter than the 90-year average for monthly precipitation totals, whilst early winter (November and December) was drier. The early months of 2007 were also slightly wetter than the 90-year average. The second set of model runs showed similar results to the first set in that vegetation reduced the overall amount of bank and toe erosion during the modeling period (Table 3; Fig. 7). The model runs carried out using the discretized flow record showed that the addition of vegetation reduced the number of large planar failures of the banks from reinforcement of the soil matrix. Small cantilever failures became the more common failure mechanism in the vegetated scenarios because of undercutting of the root zone by hydraulic scour. The majority of the modeled erosion of unvegetated banks came from large planar failures. Therefore, with addition of vegetation to the streambanks reducing such planar failures, the overall mass of material eroded from the banks was also reduced. Approximately 2.2 times more erosion was predicted for the SLR site in the unvegetated versus vegetated scenarios (1140 vs

507 m^3 , respectively, along a 100-m reach), and approximately 4.4 times more erosion was predicted for the UWH site in the unvegetated versus vegetated scenarios (1110 vs 255 m^3 , respectively, along a 100-m reach).

In the case of UWH, model runs were also performed using the regraded bank profile surveyed after vegetation was removed from this site in the late summer of 2006 (Table 3). In this set of model runs, no mass failure events were predicted, with F_s values being higher than the other scenarios with or without vegetation as the bank angles were dramatically reduced after grading. Instead, all of the predicted erosion in the regraded scenario came from toe erosion by hydraulic scour, which steepened the bank and caused the bank F_s to be reduced from 2.54 to 1.88 by the end of the modeling period. With further flow events this bank profile would continue to be steepened, eventually resulting in a cycle of failures.

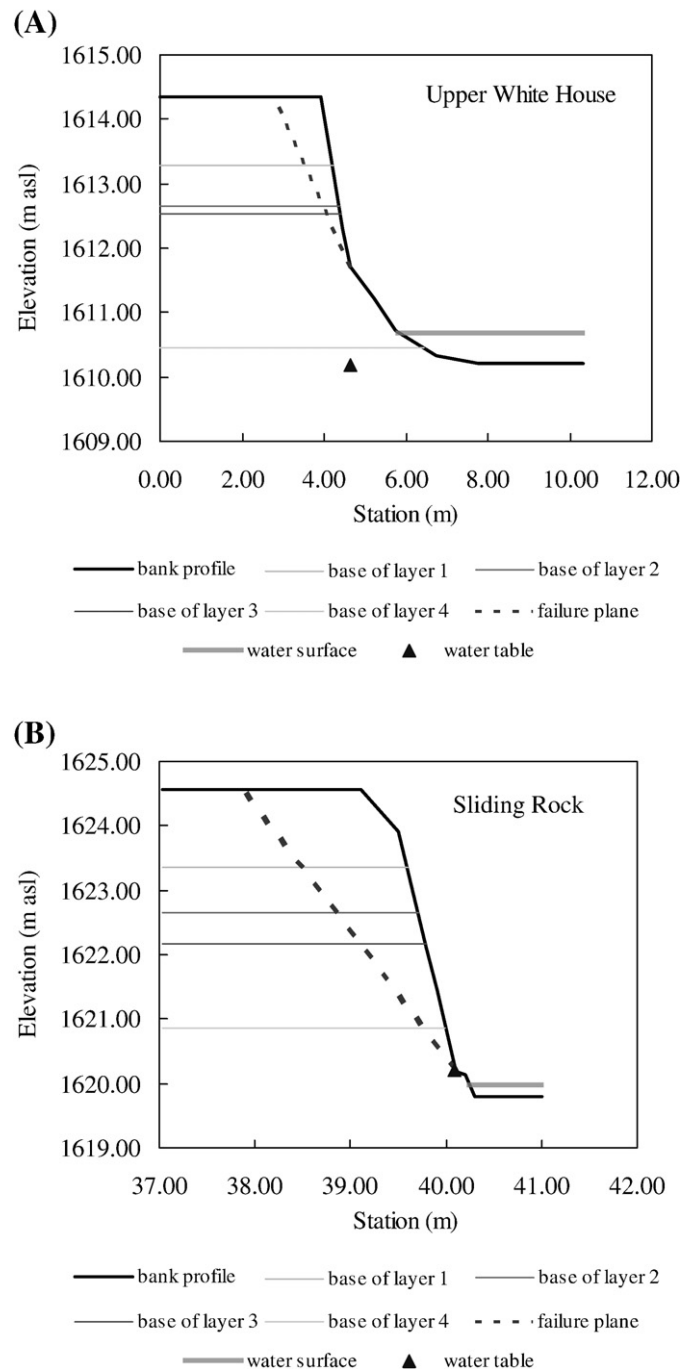


Fig. 4. Initial stable-bank configurations with vegetation for both study reaches.

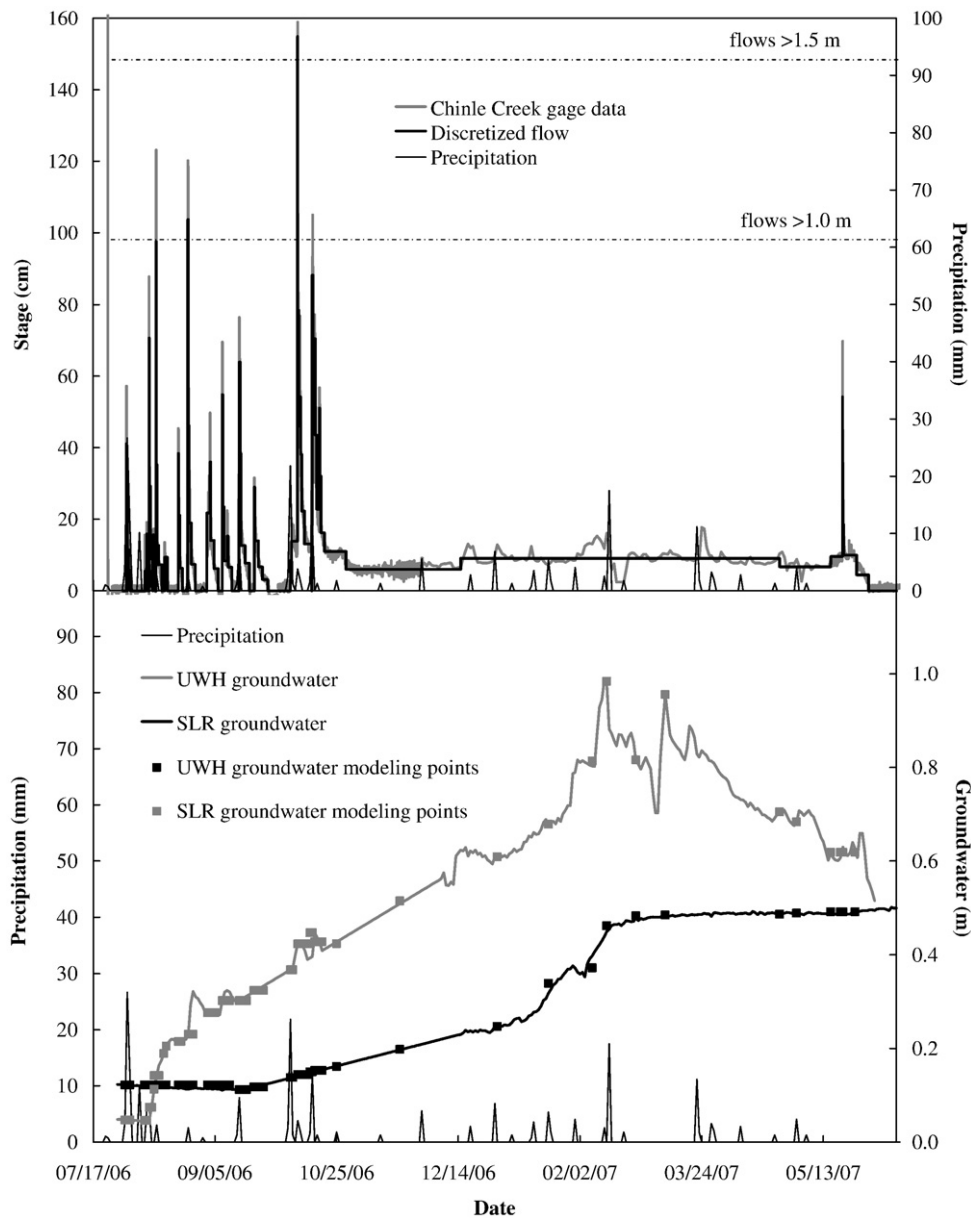


Fig. 5. Hydrologic data for modeled period (July 2006–July 2007), including precipitation, stage, groundwater elevation in wells, and discretized flow record for BSTEM modeling. For each discretized flow event the corresponding groundwater elevation was used in BSTEM.

4.3. Field observations and validation of bank erosion modeling

Dendrochronology of tilt sprouts and exposed roots provided evidence of bank failures at both sites during the 2003–2004, 2004–2005, and 2005–2006 wet seasons, indicating that channel incision has progressed to the point that the banks have become unstable under the current flow regime and vegetated conditions. In recent years, maximum amounts of bank recession on outside bends before intervention to remove invasive species were about 2.2 to 2.5 m since 2003, a rate of 0.7–0.8 m/y.

During the monitored period, both aggradation and erosion were recorded at the field sites after individual flow events. Repeat cross-sectional surveys do, however, indicate an overall trend of bank retreat, particularly on the outer bend at the UWH site. In all of the treatment reaches including the control average bank retreat at UWH was approximately 0.95 m with a maximum retreat of 2.79 m. Average bank retreat distances were smallest in the control (0.78 m) and largest in the whole plant removal reach (1.33 m). It is important to note that channel response to large flows was very localized. Immediately

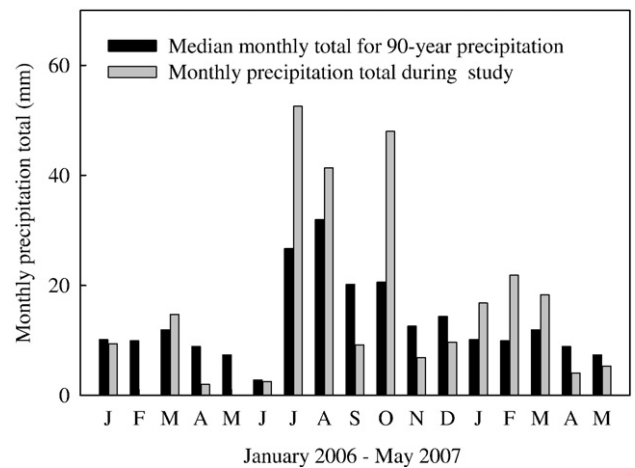


Fig. 6. Median monthly precipitation data for the 90-year data record in Canyon de Chelly, compared to the monthly precipitation totals measured between January 2006 and May 2007.

Table 2
Summary of simulation results for the UWH site showing F_s for peak flow and drawdown conditions with and without vegetation (values in bold denote simulated bank failures)

Flow #	Flow condition	F_s with vegetation	F_s without vegetation	F_s with vegetation	F_s without vegetation
		1.0-m-high flows		1.5-m-high flows	
1	@ peak	1.52	1.23	1.29	0.84
	@recession	1.52	1.23	1.29	–
2	@ peak	1.52	1.23	1.02	–
	@recession	1.52	1.17	0.89	–
3	@ peak	1.50	1.15	–	–
	@recession	1.50	1.09	–	–
4	@ peak	1.48	1.05	–	–
	@recession	1.42	0.97	–	–
5	@ peak	1.44	–	–	–
	@recession	1.44	–	–	–
6	@ peak	1.25	–	–	–
	@recession	1.11	–	–	–
7	@ peak	1.04	–	–	–
	@recession	0.94	–	–	–
8	@ peak	0.92	–	–	–
	@recession	0.84	–	–	–

downstream from the cross section modeled at UWH, the right bank retreated 4 m in the whole plant removal reach. At this location the profile scoured to a clay layer in the channel bed after an August 2007 flash flow event that reached a depth of 3.2 m. This bank retreat occurred at the apex of a meander, where hydraulic forces were maximized.

Annual surveys at the SLR site show continued incision into the clay bed in addition to channel widening. In the UWH treatment plot, the stream channel is only beginning to incise into the clay layer; the toe of the banks consists largely of silt and sand, which is less resistant than clay to erosive hydraulic forces. As a result, more stream widening is apparent in the UWH reach compared to upstream treatment plots that have become entrenched in clay. In areas, where the stream banks consist of unconsolidated silt and sand, bank retreat distances are highest and there appears to be no net bed incision.

Bank geometry profiles shown in Figs. 7 and 8 show the comparison between predicted erosion and actual erosion at the UWH and SLR sites over the modeling period. For UWH, only the model runs for the regraded bank were compared against the build surveys as the actual bank was regraded in summer 2006.

The bank at SLR was vegetated, and thus for validation purposes, the eroded areas shown in Fig. 8B should be considered. Predicted erosion from the 100-m reach of the bank at SLR with vegetation was 507 m³, whereas the repeat cross sections from surveys before and after the modeled period show that erosion during the modeled period was only 127 m³. Several modeling assumptions may help explain the discrepancies seen between predicted and actual results. First, BSTEM assumes that the bed is fixed. In reality, the bed can be eroded preferentially to the bank if the relative resistances of the bed

and bank materials are such that the bed is more erodible than the toe or bank material. The survey carried out at SLR at the end of the modeling period suggests that this indeed may be a factor in this case, as the bed elevation is lower than the starting elevation at the beginning of the modeling period (Fig. 8B). Second, BSTEM assumes that failed material is immediately transported away from the site of failure, rather than being deposited at the base of the bank. In this case, the bank survey shows that 119 m³ of material eroded from the bank face was deposited at the toe, as can be seen in the surveyed bank profile (Fig. 8B). Third, estimates of the erodibility of the bank toe materials may have been too high.

At UWH, repeat surveys carried out before and after the modeled period (after the bank had been regraded and invasive vegetation removed) indicate that BSTEM under-predicted bank erosion. In this case, actual erosion was calculated to be 459 m³ from the bank profile versus a predicted value of 208 m³ along a 100-m reach (Fig. 9). At this site, bank layering and bank material properties were tested before the bank was regraded, and the bank was found to be largely composed of sand with a layer of clay near the base of the bank. In the absence of field data pertaining to the regraded bank, the same bank layering and material properties were used in BSTEM runs for the regraded bank profile. However, the clay layer restricted toe erosion to a certain extent in the model runs, and it is possible that during regrading of the bank profile at UWH more sand was placed at the bank toe. This sand would be more easily erodible than the clay predicted to be at the toe and helps explain the discrepancy in eroded material at this site. Potential error in estimation of k values using Hanson and Simon (2001) may also have affected the simulated toe erosion, and the occurrence of bank failures during BSTEM modeling.

With the removal of invasive vegetation at the UWH site, repeated field surveys have shown that the bank face has steepened since grading, although the bank top-edge has remained fixed (Table 4). BSTEM modeling predicted similarly that the bank top-edge would remain in place, with a maximum of 1.04 m of retreat the bank face acting to increase the bank angle after grading (Table 4). A possible cause for underestimation in the model results is the difference in erodibility of intact versus reworked bank and toe materials, and uncertainty in the estimation of k values.

With vegetation removal and no regrading of the bank at UWH, the model predicted that the bank top-edge and bank face would have retreated 3.94 and 3.18 m over the same period (Table 4). With no vegetation removal and no regrading at the UWH site, the model predicted no retreat of the bank top-edge and a maximum retreat of the bank face of 0.82 m (Table 4), similar to the average rate of bank retreat observed for the control reach at UWH (0.78 m). Model results thus indicated that removal of vegetation at the UWH site may cause the rate of bank retreat to increase more than 300% with no regrading of the bank and increase by approximately 27% with vegetation removal and bank regrading. Actual bank surveys showed that removal of vegetation and regrading increased retreat of the bank face from 0.82 m/y predicted with no intervention to 1.48 m/y with

Table 3
Number of planar and cantilever failures predicted at each site during discretized bank stability modeling; also shown are erosion values for toe, bank, and total erosion under different scenarios

Site	Treatment	Number of mass failure events			Volume of eroded material from 100-m reach (m ³)			Percentage difference between treatments	
		Planar	Cantilever	Total	Toe erosion	Planar failures	Cantilever failures		Total
Upper White House	Actual erosion (graded, no vegetation)	–	–	–	–	–	–	458	120
	Modeled erosion (graded, no vegetation)	0	0	0	208	0	0	208	
	Modeled erosion (not graded, no vegetation)	2	0	2	233	878	0	1111	383
	Modeled erosion (not graded, with vegetation)	0	2	2	67	0	168	235	
Sliding Rock	Actual erosion (with vegetation)	–	–	–	–	–	–	127	
	Modeled erosion (no vegetation)	2	1	3	82	1060	1	1142	125
	Modeled erosion (with vegetation)	1	2	3	85	409	13	507	

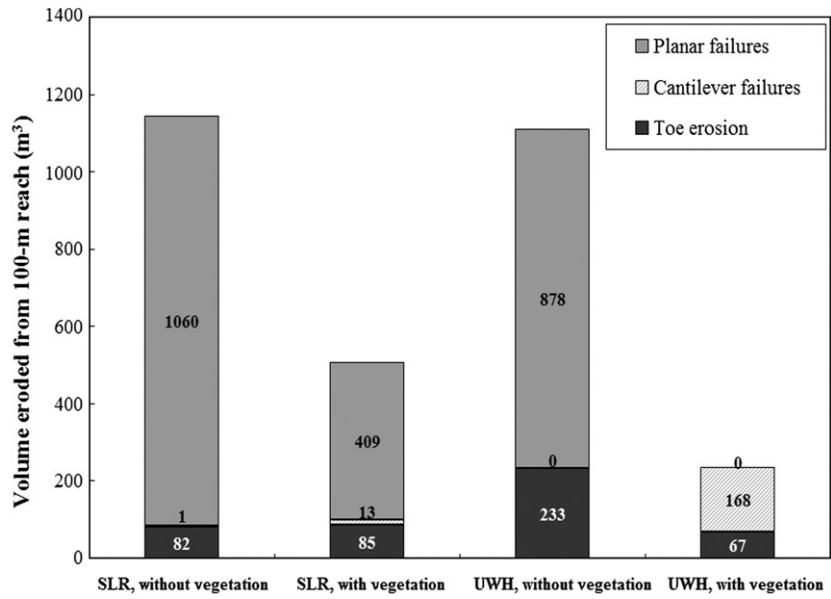


Fig. 7. Volumes of erosion predicted by BSTEM for a 100-m reach at UWH and SLR during interactive modeling of toe erosion and bank stability. Total volumes of erosion are split into that emanating from hydraulic scour of the toe versus that coming from planar and cantilever failures of the upper bank.

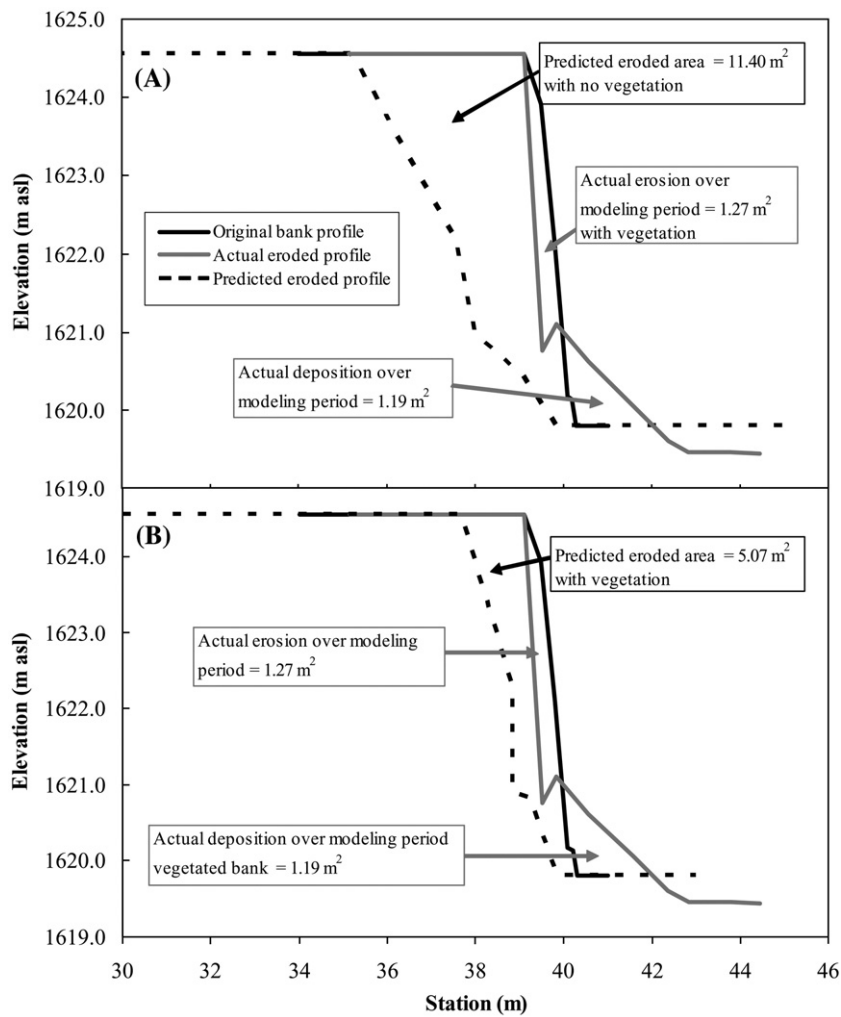


Fig. 8. Bank geometries for Sliding Rock site (SLR) at the beginning of the modeled period and after actual and predicted erosion. (A) Shows predicted erosion assuming no vegetation was present and (B) shows predicted erosion assuming Tamarisk and Russian-olive were present. In both (A) and (B) the final survey at the end of the modeled period is shown for comparison.

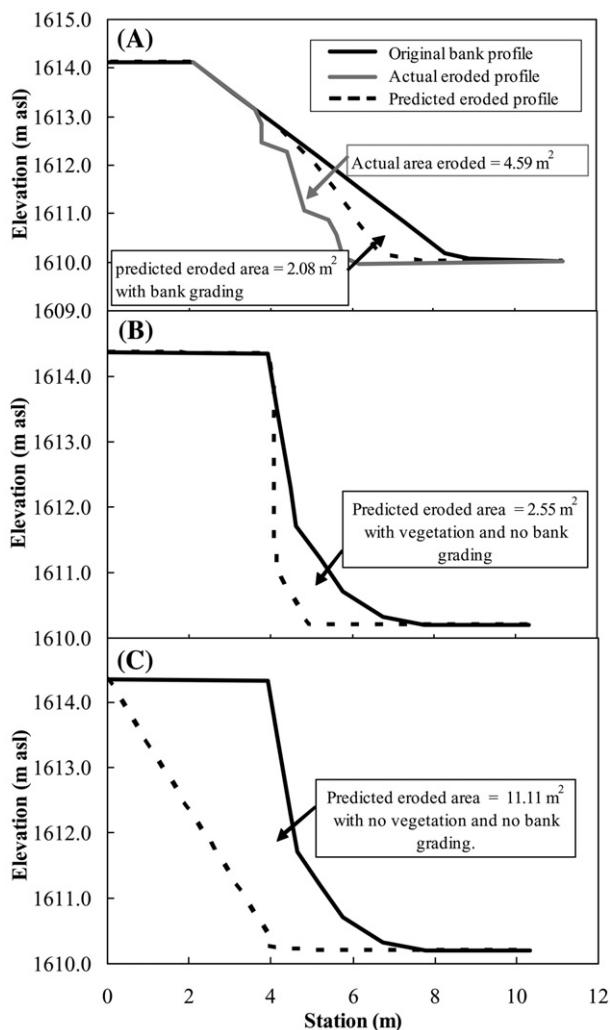


Fig. 9. Bank geometries for Upper White House site (UWH) at the beginning of the modeled period and after actual and predicted erosion. (A) Shows predicted erosion assuming no vegetation was present but the bank had been graded to a shallower angle. (B) and (C) show predicted erosion without grading of the bank with vegetation and without vegetation, respectively.

vegetation removal and regrading of the bank at the cross section modeled, an 80% increase in erosion. Field observations showed that localized bank retreat in that particular reach did, however, reach a maximum of 4 m just downstream of the modeled cross section, following an additional 3.2-m-deep flow event in August 2007. Thus, the lateral retreat rate obtained from BSTEM runs with full vegetation removal and no regrading of the bank are plausible in localized parts of the reach where the stream banks are the least resistant, as a result of substrate composition or removal of vegetation including the roots, and where hydraulic forces are maximized such as at the apex of a meander bend.

At the SLR site, where invasive vegetation was still present, the measured rate of bank retreat during the modeled period was ~0.48 m/y (Table 4). The rate of retreat obtained using BSTEM was over estimated (1.43 m/y). The removal of vegetation at SLR was predicted to increase the rate of bank retreat by about 723% from 0.48 to 3.95 m/y with no regrading of the bank (Table 4). As stated previously, overestimation of bank erosion at this site during BSTEM modeling may have been caused by the model's assumption that failed bank material is automatically removed from the bank toe at the instant of mass failure.

Still, an internally consistent set of comparisons can be made between the vegetated and non-vegetated cases given the model and

data uncertainties itemized above. Removal of vegetation at the UWH and SLR sites both result in a large increase in eroded volumes, from 120 to 383% (Table 3).

To evaluate the potential effects of a large flow event through Canyon de Chelly, one extra set of model runs was conducted for the site at UWH. Flow depth was set at the bank-top (flow depth of 4.13 m), and run through the model to simulate a 24-hour flow. Results showed that with or without vegetation, a flow event of this magnitude would cause sufficient toe erosion to undercut the regarded bank and cause mass failure resulting in bank retreat of 1.2 m. Insufficient gage data is available for Canyon de Chelly to calculate the recurrence interval of such a large flow event, but it is interesting to note that an event of this size would cause a large bank retreat, regardless of the presence or absence of riparian vegetation simply because of the amount of undercutting that was predicted to occur in these low resistance banks.

4.4. Implications of vegetation removal

Channel response and the patterns of establishment of invasive and native riparian vegetation in Canyon de Chelly are likely a result of ongoing adjustment to catchment-scale sediment and discharge conditions associated with grazing and climatic shifts over the last two centuries (Jaeger, 2008). The model runs carried out in this study consider only the short term impact of invasive vegetation removal. The model predictions and field observations after vegetation removal at UWH both show accelerated rates of widening once root-reinforcement has been removed from these banks, especially in bank materials with little inherent cohesion and/or consolidation. For how long this accelerated bank retreat will occur, and how the channel morphology as a whole will be impacted is still unknown, as the rate of bank retreat is a balance of resisting to driving forces available in the system. As such, there has to be sufficient energy available to erode the banks and bank toes, even if their resistance has been reduced by removal of vegetation. The response to vegetation removal is likely to be non-linear, with the accelerated rate of bank retreat slowing over time. As the channel widens over time, the shear stresses applied by a specific discharge will be less because of reduced flow depth in the wider channel. As a result the excess shear stress available for erosion of the bank face and toe regions will be less, and widening rates will slow down.

In addition, as widening rates decrease again, there is a greater likelihood of riparian vegetation (be it native or invasive) re-establishing itself on the banks and floodplain, creating a positive feedback in which bank retreat rates are slowed further as root-reinforcement increases again over time. Root architecture studies carried out in Canyon de Chelly as part of this study, and in other

Table 4
Measured and modeled retreat of bank edge and bank face over modeled period of one year

Site	Treatment	Maximum retreat of bank face	Maximum retreat of bank-top edge
		(m)	(m)
Upper White House	Actual erosion (graded, no vegetation)	1.48	0.00
	Modeled erosion (graded, no vegetation)	1.04	0.00
	Modeled erosion (not graded, no vegetation)	3.18	3.94
Sliding Rock	Modeled erosion (not graded, with vegetation)	0.82	0.00
	Actual erosion (with vegetation)	0.48	0.00
Sliding Rock	Modeled erosion (no vegetation)	3.54	3.95
	Modeled erosion (with vegetation)	1.43	1.43

environments have shown that whilst the roots of Tamarisk, Russian-olive, willows and cottonwoods are similar in terms of tensile strength (for more species specific tensile strength curves see Pollen and Simon, 2005), the root networks of the invasive species out compete the natives for water and tend to become more extensive those of the native species in the semi arid environment discussed here. Root-reinforcement is thus likely to be higher for re-establishing stands of invasive versus native species. Previous research on a number of riparian species growing in a range of environments has, however, indicated that relatively low amounts of root-reinforcement are provided in the first few years of growth, with values unlikely to exceed 3 kPa in even the surface layer until after 5-years of growth (Pollen-Bankhead and Simon, 2008). The same study also showed that it took seven to ten years for the reinforcing effect of a number of riparian tree species to become sufficient to stabilize the 3-m high silt bank being modeled.

5. Summary and conclusions

The results of this study have shown that BSTEM combined with RipRoot can be used in conjunction to quantify the effects of riparian species on streambank stability. Removal of the invasive species Tamarisk and Russian-olive and their root-reinforcement affects have been shown to result in increases in bank-erosion rates from 120–383%. Bank-retreat rates are predicted to increase between 300 and 723%. Uncertainties in these estimates center on issues with estimates of erodibility of the bank toe and the fate of failed material deposited at the toe.

Average root-reinforcement values over the entire bank profile were 2.5 and 3.2 kPa for Tamarisk and Russian-olive, respectively. Because the bank materials are dominated by sands, cohesion provided by roots is significant to bank stability, providing an average 2.8 kPa of cohesion to otherwise cohesionless bank materials. The removal of vegetation increased the number of large planar failures of the banks, because of reinforcement of the soil matrix. Small, cantilever failures were the more common failure mechanism in the vegetated scenarios because of undercutting of the root-zone by hydraulic scour. The majority of the bank erosion came from large planar failures.

Repeat surveys carried out at the UWH site have shown that, following removal of invasive species, bank retreat rates approximately doubled (from 0.7–0.8 m/y between 2003 and 2006 to about 1.85 m/y during the year modeled), even with the additional measure of regrading the bank profile to be a shallower angle. The field data support the BSTEM result that removal of riparian stands of Tamarisk and Russian-olive will lead to bank instabilities and accelerated widening in Canyon de Chelly National Monument.

Initial field observations following vegetation removal treatments at the UWH site indicate that flow events less than 3 m in depth resulted in only small changes in cross section geometry. In addition, the largest changes in cross section geometry occurred where the stream banks are the least resistant, as a result of substrate properties or removal of vegetation including the roots, and where hydraulic forces are maximized such as the apex of a meander bend. However, even in the presence of whole plant removal treatment, substantial geomorphic change in the stream channels is most likely to occur only as a result of repeated large flow events that exceed several meters in flow depth.

Vegetation removal along the entire riparian corridor may lead to the introduction of significantly more sediment to the system through bank widening processes, although it is not known whether this change alone would be sufficient to cause a shift in channel morphology. A shift back toward a braided channel morphology will likely require large floods or a big shift in the sediment regime of the channel. Larger flow events will be necessary to maintain rapid bank retreat. As widening rates decrease non-linearly after vegetation removal, over time, there is a greater likelihood of riparian vegetation

re-establishing itself on the banks and floodplain, further slowing retreat rates.

The ecological implications provided by the results of invasive species removal in Canyon de Chelly are directly applicable to other fluvial systems in southwestern USA where invasive species are an issue. Extrapolation to other environments is simply a matter of quantifying the root characteristics that allow quantification of root-reinforcement, and the strength of the predominant bank materials. A similar approach could be used to address the management implications of invasive species removal in other climatic zones, or conversely, the re-establishment of riparian corridors in locations where bank stabilization is desired.

The BSTEM model results presented here highlight future avenues of research that would enhance the predictive ability of the model when used iteratively over multiple storm hydrographs. Improved vegetation algorithms (Pollen-Bankhead and Simon, 2008), the fate and transport of failed material, and the addition of a near-bank groundwater model, are all features that are currently under investigation.

Acknowledgements

The authors would like to thank the staff of the NPS in Canyon de Chelly for permission to work in the canyon and for their help conducting this study. We thank Jonathan Friedman and Seth Dabney for constructive comments concerning earlier versions of this manuscript. Thanks also go to Brian Bell, Eleanor Harris, and Marianne Piggott for their help with fieldwork and data collection.

References

- Abernethy, B., Rutherford, I., 2001. The distribution and strength of riparian tree roots in relation to riverbank reinforcement. *Hydrological Processes* 15, 63–79.
- Birken, A.S., Cooper, D.J., 2006. Processes of Tamarix invasion and floodplain development along the Lower Green River, Utah. *Ecological Applications* 16 (3), 1103–1120.
- Bohm, W., 1979. *Methods of Studying Root Systems*. Springer-Verlag, Berlin.
- Busch, D.E., Smith, S.D., 1995. Mechanisms associated with the decline and invasion of woody species in two riparian ecosystems of the southwestern United States. *Ecological Monographs* 65, 347–370.
- Cadol, D.D., 2007. Aerial photographic analysis of channel change and riparian vegetation establishment in Canyon de Chelly National Monument, Arizona, 1935–2004. [M.S. thesis]: Colorado State University, 226 p.
- Everitt, B.L., 1980. Ecology of saltcedar: a plea for research. *Environmental Geology* 3, 77–84.
- Fredlund, D.G., Morgenstern, N.R., Widger, R.A., 1978. The shear strength of unsaturated soils. *Canadian Geotechnical Journal* 15, 313–321.
- Friedman, J.M., Auble, G.T., Shafroth, P.B., Scott, M.L., Merigliano, M.F., Freehling, M.D., Griffin, E.R., 2005. Dominance of non-native riparian trees in western USA. *Biol Invasions* 7, 747–751.
- Gordon, L.M., Bennett, S.J., Bingner, R.L., Theurer, F.D., Alonso, C.V., 2007. Simulating ephemeral gully erosion in AnnAGNPS. *Transactions of the ASABE*, 50 (3), 857–866.
- Graf, W.L., 1978. Fluvial adjustments to the spread of tamarisk in the Colorado Plateau region. *Geological Society of America Bulletin* 89, 1491–1501.
- Hanson, G.J., 1990. Surface erodibility of earthen channels at high stresses. Part II: Developing an in-situ testing device. *Transactions of the ASAE* 33 (1), 132–137.
- Hanson, G., Simon, A., 2001. Erodibility of cohesive streambeds in the loess area of the Midwestern USA. *Hydrological Processes* 15 (1), 23–38.
- Hupp, C.R., Osterkamp, W.R., 1996. Riparian vegetation and fluvial geomorphic processes. *Geomorphology* 14 (4), 277–295.
- Knapen, A., Poesen, J., Govers, G., Gyssels, G., Nachtergaele, J., 2007. Resistance of soils to concentrated flow erosion: a review. *Earth Science Reviews* 80, 75–109.
- Langendoen, E.J., Simon, A., 2008. Modeling the evolution of incised streams: II. Streambank erosion. *Journal of hydraulic engineering* 134 (7), 905–915.
- McPherson, R.S., 1998. Navajo livestock reduction in southeastern Utah, 1933–46: history repeats itself. *American Indian Quarterly* 22, 1–18.
- Osterkamp, W.R., Costa, J.E., 1987. Changes accompanying an extraordinary flood on a sand-bed stream. In: Mayer, L., Nash, D. (Eds.), *Catastrophic Flooding*. Allen and Unwin, Boston, Massachusetts, USA, pp. 201–224.
- Partheniades, E., 1965. Erosion and deposition of cohesive soils. *Journal of the Hydraulics Division, Proceedings of the American Society of Civil Engineers*. 91 (1), 105–139.
- Pollen, N., 2007. Temporal and spatial variability in root reinforcement of streambanks: accounting for soil shear strength and moisture. *Catena* 69, 197–205.
- Pollen-Bankhead, N.L., Simon, A., 2008. Enhanced application of root-reinforcement algorithms for bank-stability modeling. *Earth Surface Processes and Landforms*. available online July 2008.
- Pollen, N., Simon, A., 2005. Estimating the mechanical effects of riparian vegetation on streambank stability using a fiber bundle model. *Water Resources Research* 41, W07025, doi:10.1029/2004WR003801.
- Schumm, S.A., Lichty, W., 1963. Channel widening and floodplain construction along Cimarron River in southwestern Kansas. *US Geological Survey Professional Paper* 352-D, p. 88.

- Selby, M.J., 1982. *Hillslope Materials and Processes*. Oxford University Press, Oxford, p. 54.
- Simon, A., Collison, A.J.C., 2002. Quantifying the mechanical and hydrologic effects of riparian vegetation on streambank stability. *Earth Surface Processes and Landforms* 27, 527–546.
- Simon, A., Thomas, R., 2002. Processes and forms of an unstable alluvial system with resistant, cohesive streambeds. *Earth Surface Processes and Landforms* 27, 699–718.
- Simon, A., Curini, A., Darby, S.E., Langendoen, E.J., 2000. Bank and near-bank processes in an incised channel. *Geomorphology* 35, 183–217.
- Simon, A., Pollen, N., Langendoen, E.J., 2006. Influence of two woody riparian species on critical conditions for streambank stability: Upper Truckee River, California. *Journal of American Water Resources Association* 42 (1), 99–113.
- Simon, A., Pollen, N., Jaeger, K., Wohl, E., 2007. Implications for the removal of invasive species in Canyon de Chelly National Monument. *Proceedings of ASCE-EWRI conference*, Tampa, May 2007.
- Travis, T.E., 2007. *Continuity and change in the Navajo community of Canyon del Muerto and de Chelly*. Dissertation. Arizona State University, Tempe, Arizona. 225 pp.
- Tooth, S., Nanson, G.C., 1999. Anabranching rivers on the Northern Plains of arid central Australia. *Geomorphology* 29, 211–233.
- Tooth, S., Nanson, G.C., 2000. The role of vegetation in the formation of anabranching channels in an ephemeral river, Northern Plains, arid central Australia. *Hydrological Processes* 14, 3099–3117.
- Weisiger, M.L., 2000. *Dine Bikeyah: environment, cultural identity, and gender in Navajo country*. Dissertation. University of Wisconsin, Madison, WI. 248 pp.
- Wu, T.H., McKinnell III, W.P., Swanston, D.N., 1979. Strength of tree roots and landslides on Prince of Wales Island, Alaska. *Canadian Geotechnical Journal* 16, 19–33.
- Wynn, T., Mostaghimi, S., 2006. Effects of riparian vegetation on stream bank subaerial processes in southwestern Virginia, USA. *Earth Surface Processes and Landforms* 30 (4), 399–413.